Decoupling Surface Production from Deep Remineralization and Benthic Deposition: Empirical Evidence and Modeling Challenges

by

Robert A. Armstrong
Marine Sciences Research Center
Stony Brook University
Stony Brook, NY 11794-5000
rarmstrong@notes.cc.sunysb.edu

Two views of deep remineralization: export-driven vs. ballast-driven

- Export-driven. Assumption: that particulate organic carbon (POC) fluxes at depths $z > z_0$ are determined uniquely by the POC flux at some "export horizon" z_0, independent of any other factors:

$$F_{OC}(z) = F_{OC}(z_0)\ f(z, z_0)\ .$$

Example: the "Martin curve"

$$F_{OC}(z) = F_{OC}(z_0)\ (z / z_0)^{\beta}\ .$$

- Ballast-driven. Assumptions: (1) that there are two dominant components to POC flux, one quantitatively associated (QA) with, and perhaps protected by, ballast (silicate and carbonate minerals, and dust) flux $F_B(z)$:

$$F_{OC}^{QA} = (OC : B)_{\infty}\ F_B(z)\ .$$

(2) That the remaining flux of "excess" (E) POC is remineralized as a function of depth only:

$$F_{OC}^{E}(z) = F_{OC}^{E}(z_0)\ f_E(z, z_0)\ .$$

Together, the total flux is

$$F_{OC}(z) = F_{OC}^{QA}(z) + F_{OC}^{E}(z)\ .$$

Export-driven and ballast-driven models of deep-water remineralization

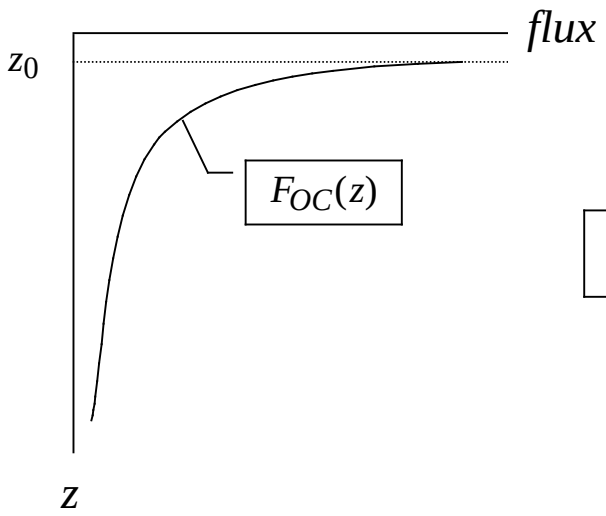

Export-driven

$$F_{OC}(z) = F_{OC}(z_0) \quad f(z, z_0)$$

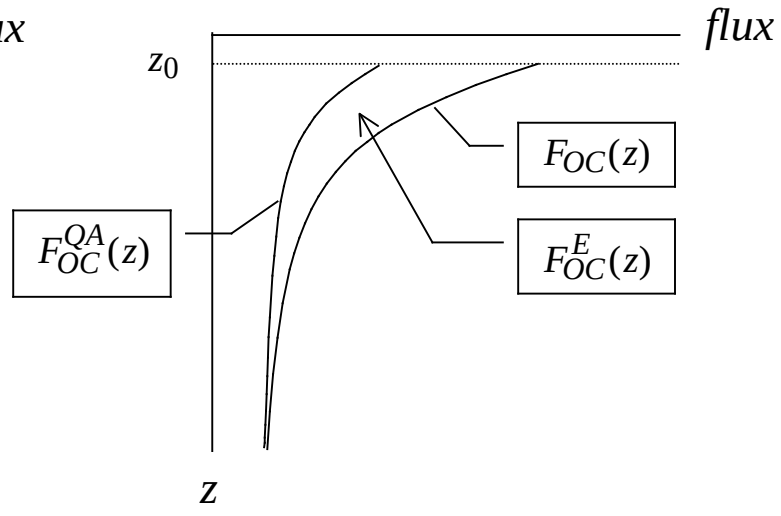

Ballast-driven

$$F_{OC}(z) = F_{OC}^{QA}(z) + F_{OC}^{E}(z)$$

$$F_{OC}^{QA}(z) = (OC:B)_{\infty} \quad F_B(z)$$

$$F_{OC}^{E} = (F_{OC}(z_0) - (OC:B)_{\infty} \quad F_B(z_0)) \quad f_E(z, z_0)$$

Support for the ballast model

- Armstrong et al. (2002, DSR II 49:219) confronted a set of export-driven and ballast-driven models with data from the US JGOfS EqPac study. In this comparison, ballast-driven models were statistically superior to models without ballast at $p<0.005$.

- Additional insight into the ballasting hypothesis comes from rearranging the ballast equations as

$$\begin{aligned} F_{OC}^{E}(z) &= F_{OC}(z) - F_{OC}^{QA}(z) \\ &= F_{OC}(z) - (OC:B)_{\infty}\ F_{B}(z) \end{aligned} .$$

  Since $F_{OC}(z)$ and $F_{B}(z)$ are data, we can plot the estimate $\hat{F}_{OC}^{E}(z)$ of excess POC against depth. To allow plotting all data on the same graph, we normalize excess fluxes from location (latitude) *i* by an estimate of total POC flux through the export horizon $\hat{F}_{OC,i}(z_0)$ for that location:

$$\hat{F}_{OC,i}^{E}(z) / \hat{F}_{OC,i}(z_0) .$$

  Finally, we assume that the asymptotic transport ratio $(OC:B)_{\infty}$ for EqPac is 0.051 (Armstrong et al. 2002).

- The resulting best fit to a power function, with $\beta = -0.90$,

$$F_{OC}^{E}(z) / F_{OC}(z_0) = (z/105)^{-0.90} ,$$

  is statistically indistinguishable from the best fit to an exponential with length scale 600 m:

$$F_{OC}^{E}(z) / F_{OC}(z_0) = \exp((z-105)/600) .$$

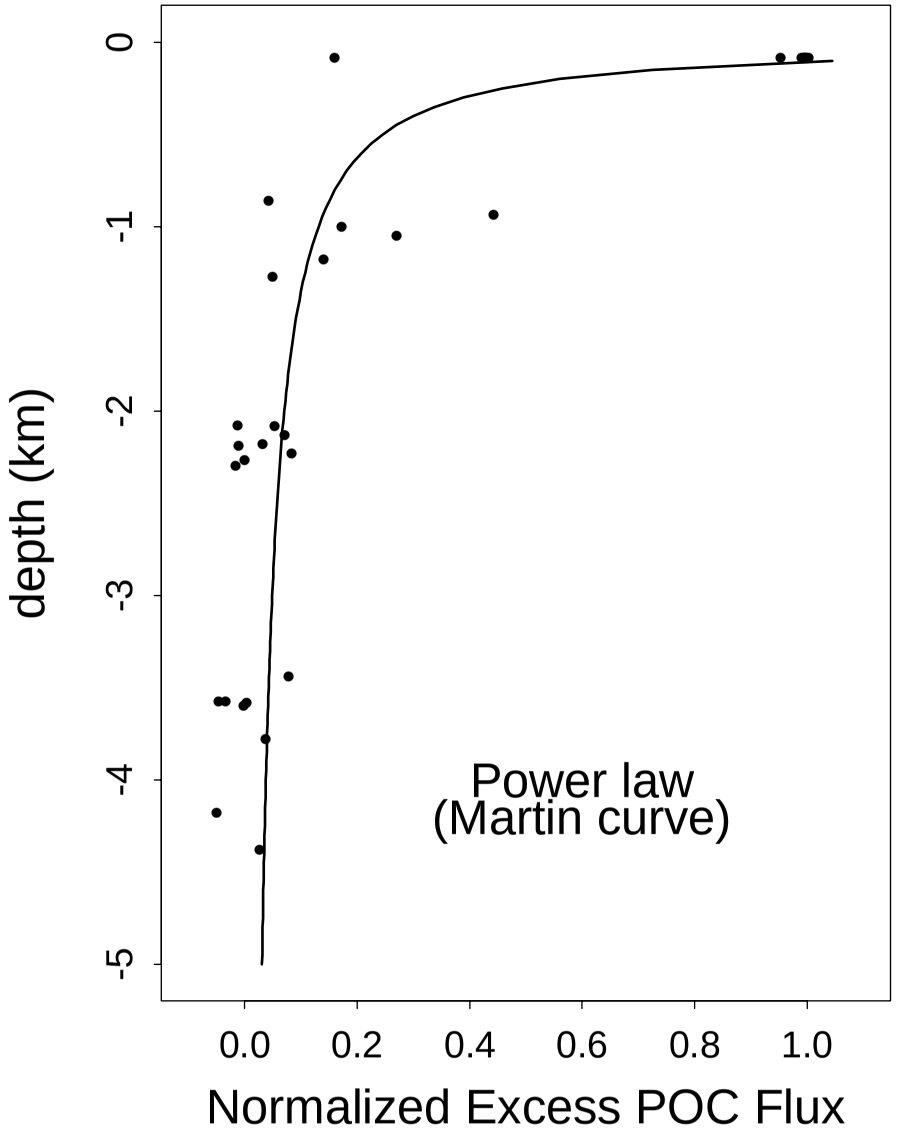
depth (km)
0
-1
-2
-3
-4
-5
0.0
0.2
0.4
0.6
0.8
1.0
Normalized Excess POC Flux
Power law
(Martin curve)

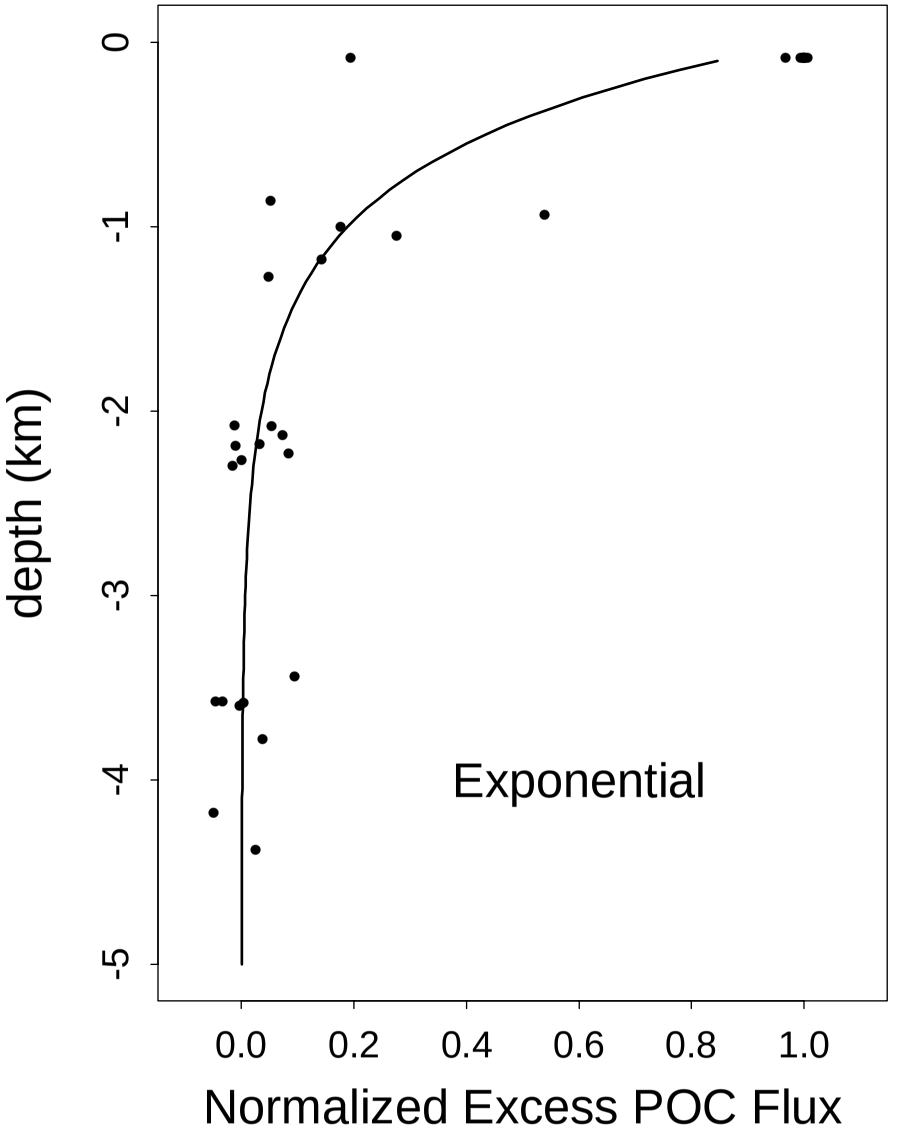
depth (km)
0
-1
-2
-3
-4
-5
0.0
0.2
0.4
0.6
0.8
1.0
Normalized Excess POC Flux
Exponential

Empirical Summary and Modeling Challenges

1. These preliminary results are being implemented in several global General Circluation Models (Caldeira, Doney/Moore, Klaas, Sarmiento), but further work is needed. An example is provided in the preceding viewgraph: there are not enough data in the mesopelagic ("twilight zone") to distinguish exponential curves of "excess" POC from power laws (or from anything else!)

2. Fits to flux data can only get us so far: we need more mechanistic understanding
   - Is it "protection"? Or is it "glue"?
   - Is it surface area of particles? Or is it particle composition?

3. This mechanistic knowledge will be crucial in making models for prediction
   - Informs the choice of a successor to the Martin curve
   - In doing so, drives the form of photic zone ecosystem models and models of the mesopelagic

A model structure for analysis of food web data and for carbon cycle simulation

by

Rob Armstrong
Marine Science Research Center
Stony Brook University
Stony Brook, NY 11733

Motivations

- Previous size-structured models of marine food webs have proved inadequate for analyzing food web data. In particular, the use of discrete, non-overlapping "boxes" for size classes does not capture the size plasticity of individual organisms, nor does it reflect the fact that characteristic size differences among competing species may not be the same as characteristic size differences between adjacent trophic levels.

- Simulation models are only as good as the data on which they are based; therefore, where possible, data should be analyzed using models that are also capable of use in simulations.

Reference: Armstrong, R.A. Beyond Moloney and Field: A hybrid spectral model of plankton interaction. DSR II (submitted)

Figure Legends

Fig 1. The model of Moloney and Field (1991). Discrete size classes of phytoplankton are often identified with prominent phytoplankton taxa such as *Prochorococcus* ("*Pro*"), *Synechococcus* ("*Syn*"), and diatoms, though this classification belies the true complexity of both phytoplankton and zooplankton communities (cf. Figs 5 and 6 below).

Fig. 2. The proposed model. Zooplankton abundance is represented by the continuous size spectrum $\zeta(x')$; densities of phytoplankton and bacterial species are denoted $\rho(x)$.

Fig. 3. Dynamics of discrete phytoplankton/bacterial size classes p_i are determined by dynamical equations

$$\frac{1}{p_i}\frac{dp_i}{dt} = \mu_i(N,T) - \sum_j a_{ij} z_{ij} p_j \ ,$$

where $\mu_i(N,T)$ is the growth rate of species *i* as a function of nutrients *N* and temperature *T*; the a_{ij} represent overlaps among

phytoplankton/bacterial size classes ($a_{ij} \rightarrow 1$ as the sizes of species *i* and *j* become more similar); and the z_{ij} are "effective" densities of herbivorous zooplankton determined from the zooplankon size spectrum. The model contains prescriptions for calculating these quantities from data and during simulations.

Fig. 4. A simulated "bloom" of species in IronEx II. Upper panel: phytoplankton growth rate was assumed to have the illustrated form before the addition of iron, and was assumed to be constant ($\mu_i = \mu_{max}$ for all *i*: no nutrient limitation) after addition of iron. Middle panel: zooplankton density increase during the bloom was modeled from data in Landry et al. (2000. MEPS 201:27-42). Bottom panel: the resulting phytoplankton bloom.

Fig. 5. Fits of the model simulation to phytoplankton abundances from Landry et al. (2000). Note that each size class may contain multiple taxonomic types.

Fig. 6. Fits of the model simulation to zooplankton abundance from Landry et al. (2000). Each size class may contain multiple taxonomic types.

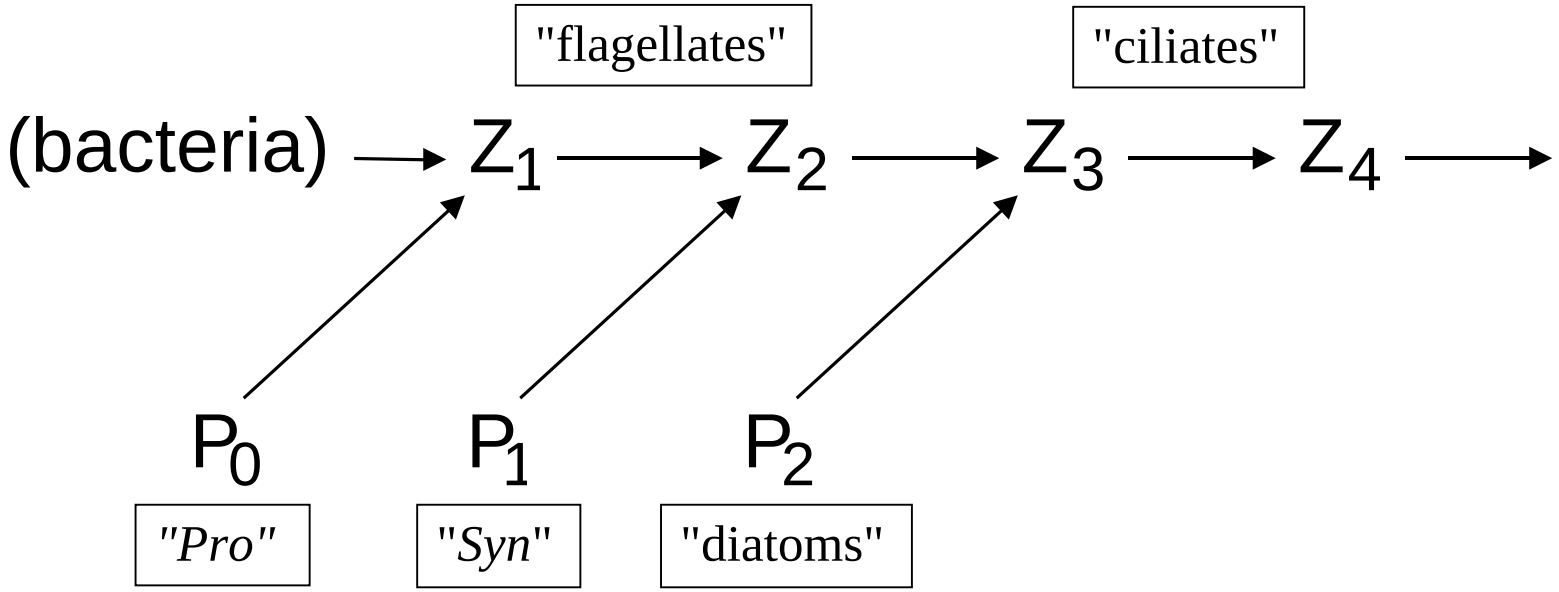

Figure 1. The model of Moloney and Field (1991)

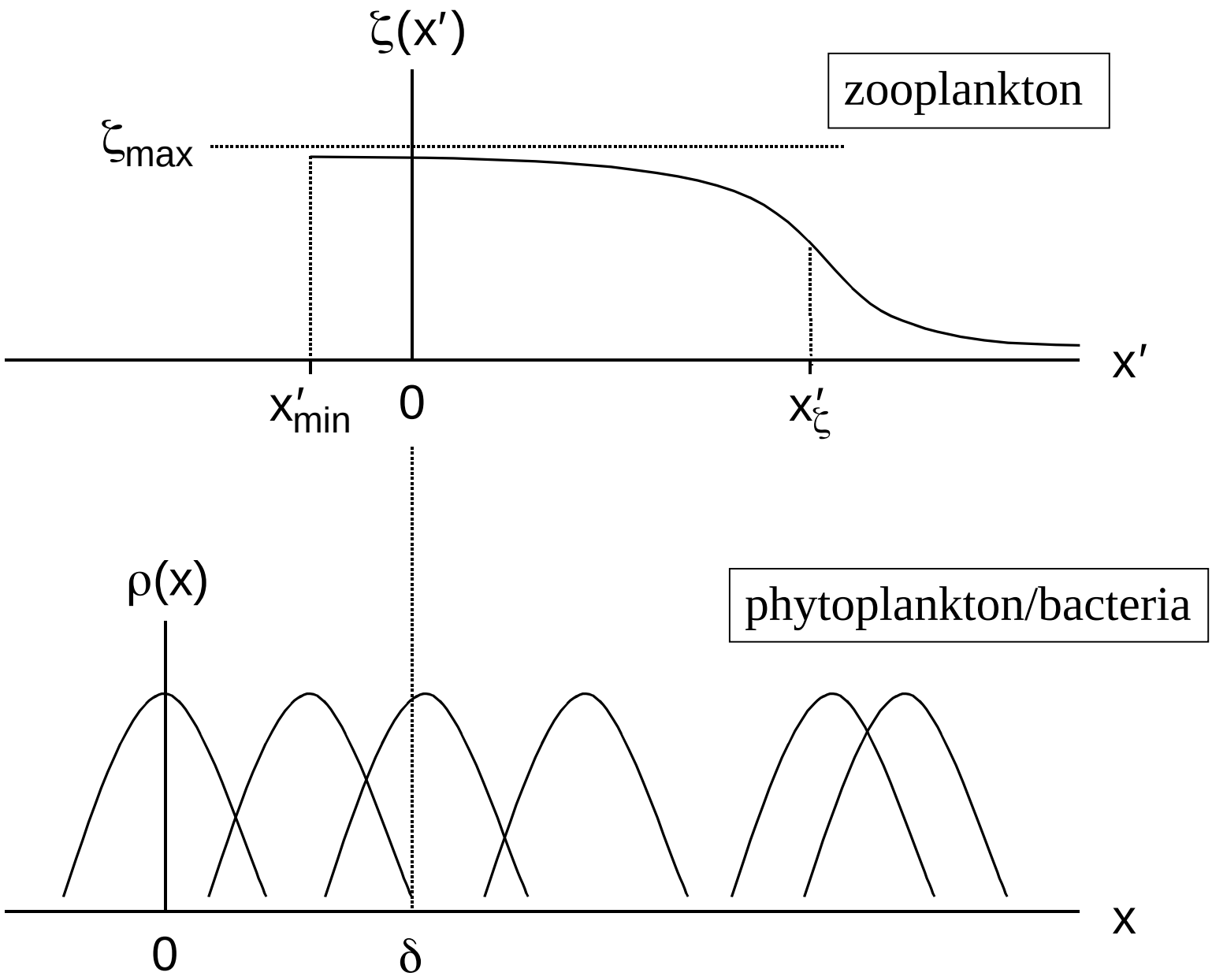

Figure 2: Structure of the present model (DSR II submitted)

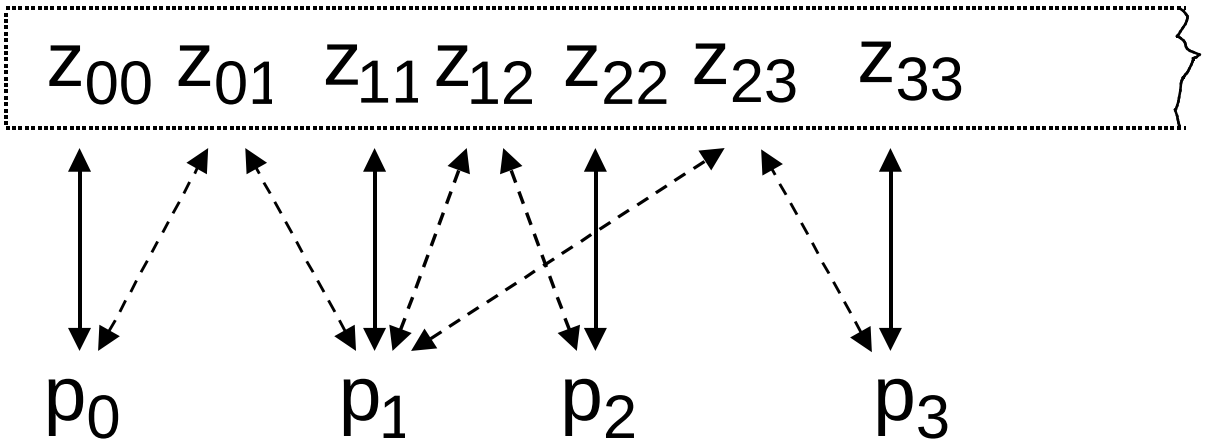

Figure 3: Relationships among state variables
in the present model (DSR II submitted)

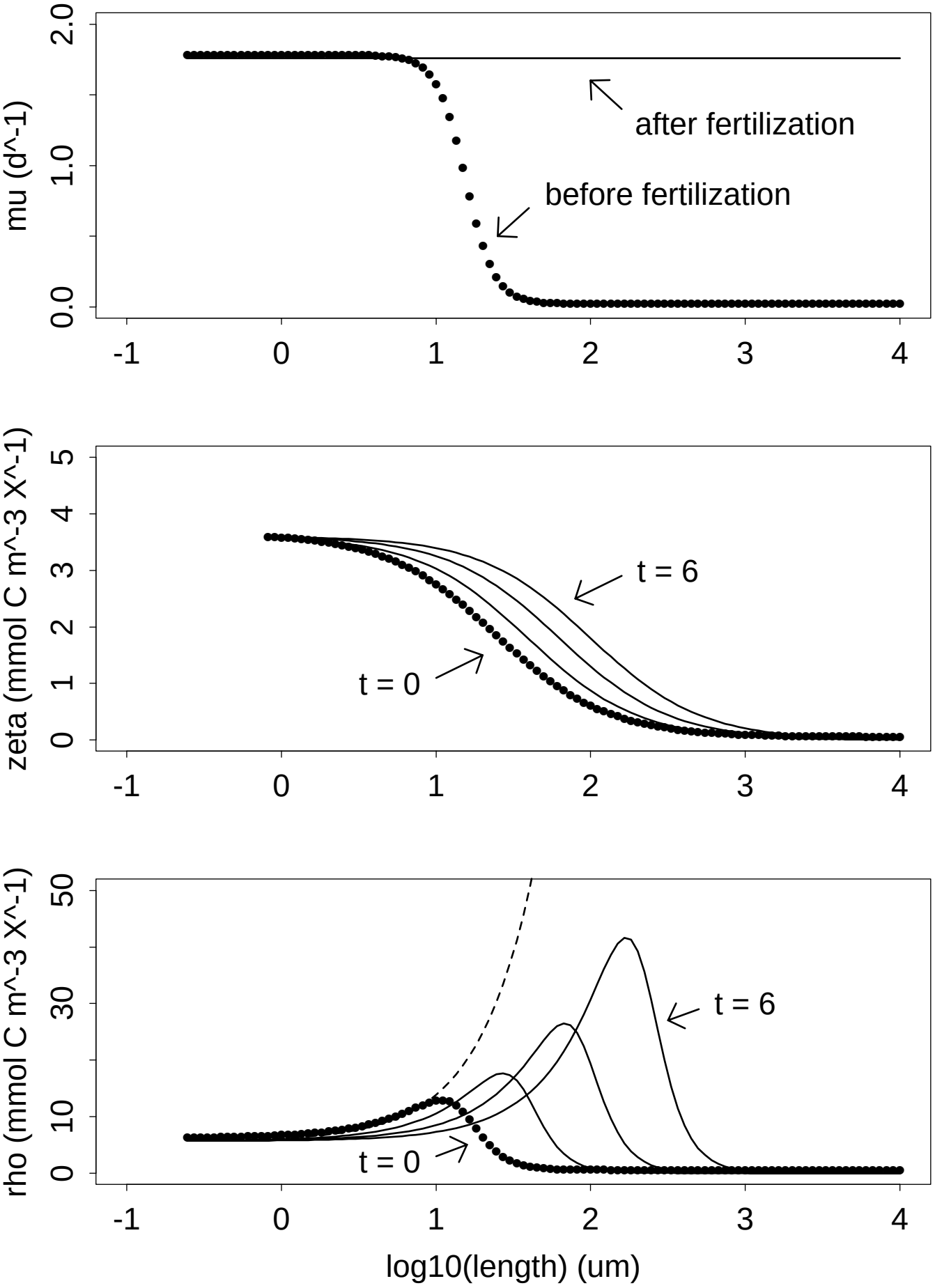

Figure 4: Application to IronEx II

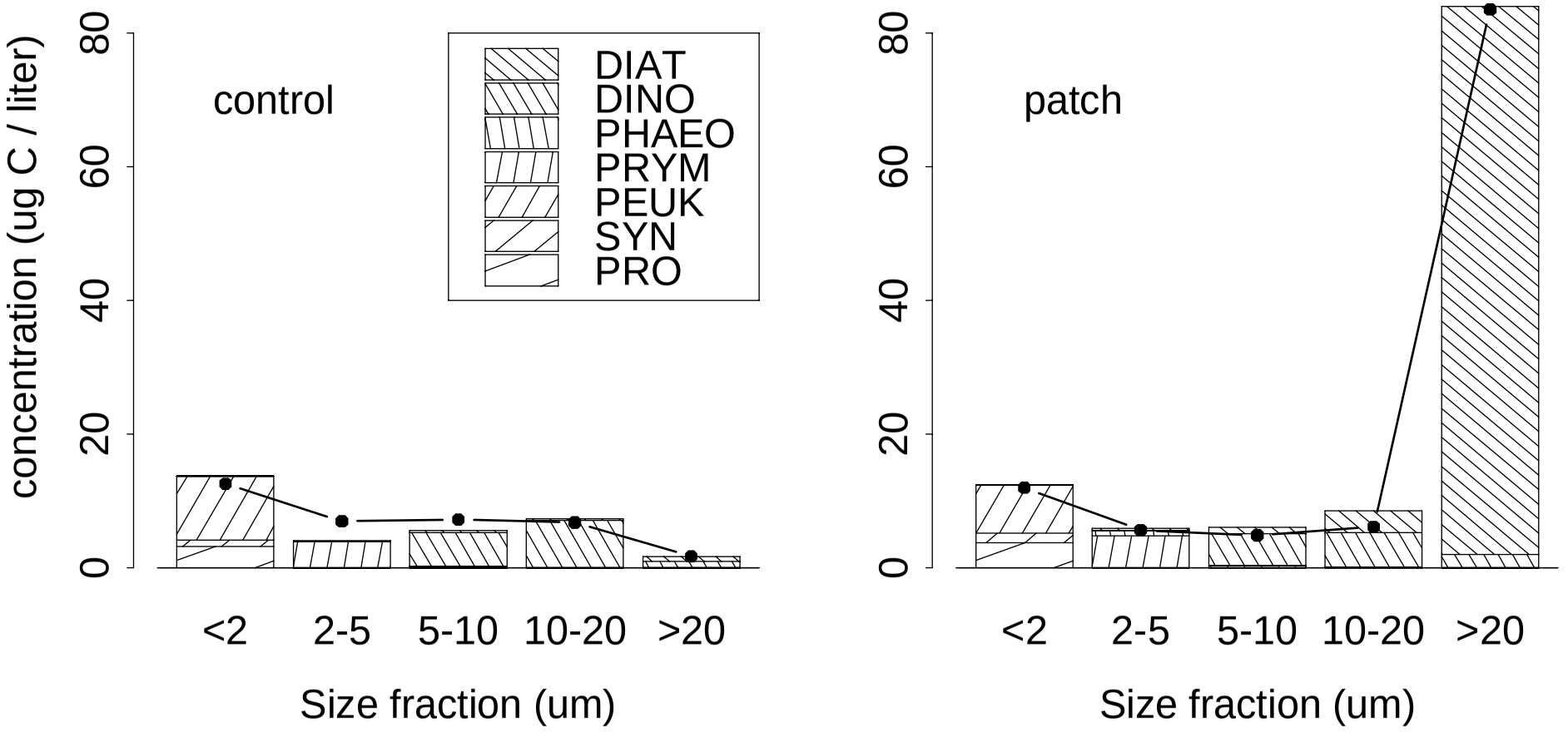

Figure 5: Phytoplankton in IronEx II

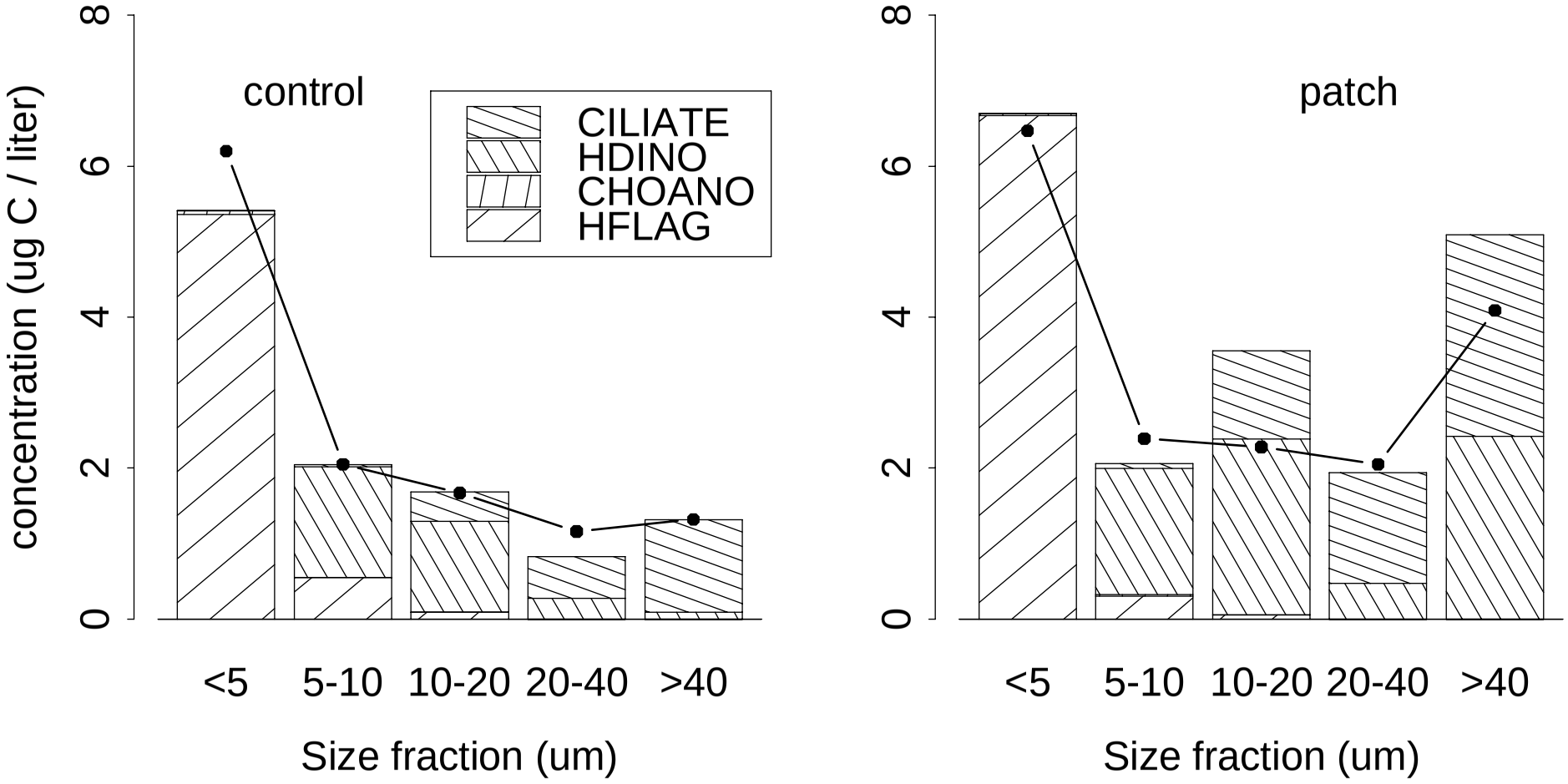

Figure 6: Zooplankton in IronEx II